

Collaborative Neural Rendering using 2D Anime Character Sheets

Zuzeng Lin^{1,2,*} Ailin Huang^{1,3,*} Zhewei Huang^{1,*}

Chen Hu¹ Shuchang Zhou¹

¹Megvii Inc ²Tianjin University ³Wuhan University

transpchan@gmail.com, {huangailin, huangzhewei, huchen, zsc}@megvii.com

Abstract

Drawing images of characters with desired poses is an essential but laborious task in anime production. In this paper, we present the Collaborative Neural Rendering (CoNR) method to create new images from a few reference images with various poses, namely Character Sheets. In general, the high diversity of body shapes of anime characters defies the employment of universal body models for real-world humans, like SMPL. To overcome this difficulty, CoNR uses a compact and easy-to-obtain landmark encoding to avoid creating a unified UV mapping in the pipeline. In addition, the performance of CoNR can be significantly improved when referring to multiple reference images and using feature space cross-view warping in a carefully designed neural network. Moreover, we collected a character sheet dataset containing over 700,000 hand-drawn and synthesized images of diverse poses to facilitate research in this area. Our code and demo are available at <https://github.com/megvii-research/CoNR>.

Introduction

2D Animation is one of the essential carriers of art reflecting human creativity. Human artists commonly use character sheets to show their virtual character design. A character sheet is the image collection of a specific character with multiple postures observed from different viewpoints. It covers all the appearance details and is widely used to assist the creation of animations or their derived media. Moreover, character sheets allow many artists to cooperate while maintaining the consistency of the design of this character.

Drawing a sequence of anime frames is extremely time-consuming, requiring imagination and expertise. Due to the semantic gap between the character sheet and the desired poses, it is challenging for computers to draw character images automatically. Non-photorealistic rendering (Gooch and Gooch 2001) methods can simulate the artistic style of hand-drawn animation. For example, Toon Shading is currently widely used in games and animation production. Still, it requires a very complex manual design to approximate a specific artistic style, which is too complicated for animators and painters.

We formulate the task of rendering a particular character in the desired pose from character sheets. We consider character sheets as dynamical-sized sets to fit a wider range

of input situations. Based on this formulation, we develop a **Collaborative Neural Rendering (CoNR)** model based on convolutional neural network (CNN). CoNR fully exploits the information available in a provided set of reference images by using feature space cross-view dense correspondence and warping. In addition, CoNR uses the Ultra-Dense Pose (UDP), an easy-to-construct compact landmark encoding tailored for anime characters to avoid requiring a unified UV texture mapping (Yao et al. 2019; Yoon et al. 2021; Gao et al. 2020) in the pipeline. It can represent the fine details of characters, such as accessories, hairstyles, or clothing, thus allowing better artistic control. It can also be easily generated with existing computer graphics pipelines, allowing a wide range of interactive applications. Moreover, we collected a character sheet dataset containing over 700,000 hand-drawn and 3D-synthesized images of diverse poses and appearances (which will be released). Training on this dataset, CoNR achieves impressive results both on hand-drawn and synthesized images.

To sum up, our main contributions are:

- We formulate a new task, rendering 2D anime character images with desired pose using character sheets.
- We introduce a UDP representation for anime characters and build a large character sheet dataset containing diverse poses and appearances.
- We explore a multi-view collaborative inference model, CoNR, to produce impressive generative effects. CoNR is considerable potential to assist in anime video creation.

Related Work

Image Generation and Translation for Anime

Recent years have seen significant advancement in applying deep learning methods to assist the creation of anime. For example, (Gao et al. 2018; Zheng, Li, and Bargteil 2020) propose to apply realistic lighting effects and shadow for 2D anime automatically; (Wang and Yu 2020a) propose to transfer photos to anime style; (Siyao et al. 2021) propose to interpolate in-between frames for anime. There are also attempts to produce vectorized anime images (Su et al. 2021), similar to the step-by-step manual drawing process. The generative modeling of anime faces has achieved very impressive results (Jin et al. 2017; Gokaslan et al. 2018; Tseng et al. 2020; Li, Jin, and Zhu 2021; He, Kan, and Shan 2021).

*These three authors contribute equally to this work

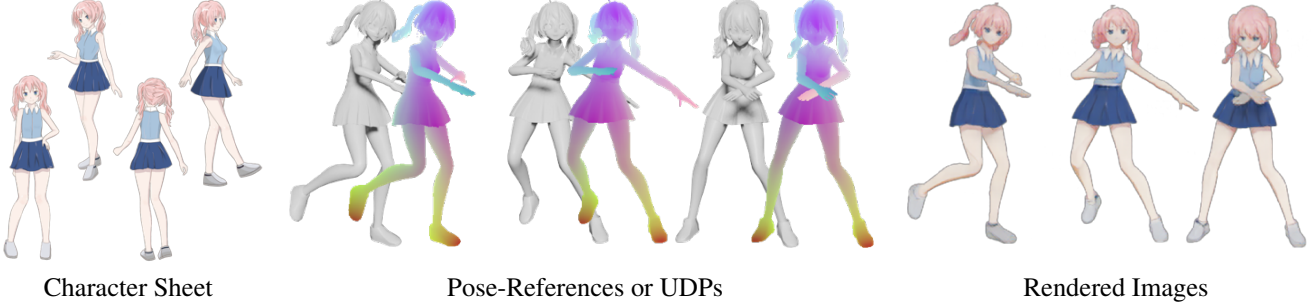


Figure 1: **The overview of CoNR.** CoNR takes several reference images designed by artists as the character sheet input, and UDPs as the pose input. Then, the model renders an image of the given character with the desired pose

The latent semantics of generative models has also been extensively explored (Shen and Zhou 2021). A modified StyleGAN2 model (aydao 2021) is proven to be able to generate full-body anime images, although it still suffers from artifacts because of the high degree of freedom of the human body.

Representation of Human Body

Stick-figure of skeletons (Chan et al. 2019), SMPL vectors (Loper et al. 2015), and heat maps of joints (Cao et al. 2019; Siarohin et al. 2021) are widely-used representations obtained from motion capture system. However, when these sparse representations are used for anime characters (Khungurn and Chou 2016), they face a new series of challenges: noisy manual annotations, unexpected occlusions caused by the wide variety of characters’ clothing and body shapes, and ambiguity due to hand drawing. Furthermore, the aforementioned human pose representations only represent human joints and body shapes. However, anime characters often require flexible artistic control over other body parts, such as the fluttering of hair and skirts. These representations cannot directly drive these parts.

Human parsers or clothing segmenters (Zanfir et al. 2018; Yoon et al. 2021; Gafni, Ashual, and Wolf 2021; Chou et al. 2021) are robust to the uncertainty of joint positions. However, the provided semantic masks are not informative enough to represent the pose or even the orientation of a person. DensePose (Güler, Neverova, and Kokkinos 2018) and UV texture mapping (Yao et al. 2019; Yoon et al. 2021; Gao et al. 2020), greatly enhance the detail of pose representation on the human body or face by adding a universal definition that essentially unwarps the 3D human body surface into a 2D coordinate system. However, due to the great diversity and rich topology of anime characters, it is difficult to find a general labeling method to unwarp them, which makes existing dense representations still not serve as an off-the-shelf solution for anime-related tasks.

There are also some dense representations of the body, such as CSE (Neverova et al. 2020). CSE addresses the task of detecting a continuous surface coding from an image. Similar “define-by-training” methods are inapplicable in anime creation since CSE can only be used for reenactment currently.

Human Appearance Transfer

Most of works create vivid body motions or talking heads from only one single image (Yao et al. 2019; Gafni, Ashual, and Wolf 2021; Sarkar et al. 2020; Wang, Mallya, and Liu 2021; Yoon et al. 2021; Siarohin et al. 2019; Liu et al. 2019). The learned prior of the human body (Loper et al. 2015), head (Blanz and Vetter 1999), or real-world clothing shape and textures (Alldieck et al. 2019) enable the model to solve ill-posed problems like imagining and inpainting the back view even if only the frontal view is available. However, anime has long been featuring a flexible character design leading to high diversity in clothing, body shapes, hairstyles, and other appearance features. A model trained on a huge dataset (e.g., CLIP (Radford et al. 2021)) might be able to encode some popular anime character designs implicitly, but it is generally more challenging to establish priors or styles in the anime character domain than that in the real human domain.

There are also some attempts (Liu et al. 2021) to extend the pose transfer task by utilizing SMPL (Loper et al. 2015), a realistic 3D mesh of the naked human body that is based on skinning and blend-shapes, to combine appearance from different views. Using multiple reference images would, in principle, allow the model to follow the original appearance of the given person and better suit the needs of anime production.

Some recent works utilize neural rendering models (Mildenhall et al. 2020) which are trained using photometric reconstruction loss and camera poses over multiple images of 3D objects and scenes. Due to their ray-marching nature and capability to in-paint in 3D, they are promising methods in modeling real-world 3D data (Pumarola et al. 2021; Peng et al. 2021). These methods are not influenced by or depend on prior knowledge other than the object to be modeled. However, they have not yet made much progress in modeling hand-drawn data like anime character sheets, which less follow strict geometric and physical constraints.

Method

Task Formulation

Our formulation is similar to the tasks about drawing or painting art (Zhang et al. 2009; Huang, Zhou, and Heng

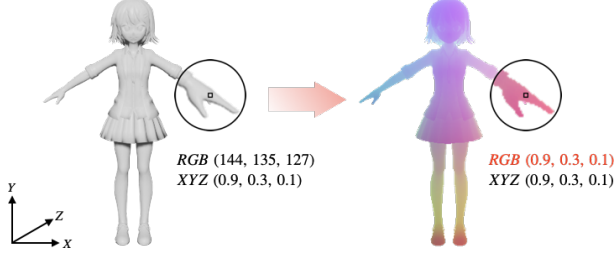


Figure 2: **UDP representation of a random anime character (Kurei Kei).** UDP uses 3D coordinates at same **A-pose** as landmarks. When the anime body changes its pose, the landmark at the corresponding body part will remain the same. Compared to existing dense human-pose representations, UDP bypasses the step of unwarping 3D surfaces onto a 2D UV texture mapping, which may not be done in a consistent method for anime characters

2019; Su et al. 2021). We consider the character sheet $I_n \in S_{ref}$ in a whole. A target pose P_{tar} representation is also required in the input to provide rendering directives to the model. The task can be formulated as mapping S_{ref} to target image \hat{I}_{tar} with the desired target pose P_{tar} :

$$\hat{I}_{tar} = \Phi(P_{tar}, S_{ref}). \quad (1)$$

We notice that complicated poses, motions, or characters may require more references in S_{ref} than others, so dynamically sized S_{ref} should be allowed.

Ultra-Dense Pose

A UDP specifies a character’s pose by mapping 2D view-port coordinates to feature vectors, which are 3-tuple floats that continuously and consistently encode body surfaces. In this way, a UDP can be represented as a color image $P_{tar} \in \mathbb{R}^{H \times W \times 3}$ with pixels corresponding to landmarks $L_{(x,y)} \in \mathbb{R}^3$. Non-person areas of the UDP image are masked. It allows better compatibility across a broader range of anime body shapes and enables better artistic control over body details like garment motions.

3D meshes are widely used data representations for anime characters in their game adaptations. Vertex in a mesh usually comprises corresponding texture coordinate (u, v) or a vertex color (r, g, b) . Interpolation over the barycentric coordinates allows triangles to form faces filled with color values or pixels looked up from textures coordinates.

Taking a bunch of anime body meshes standing at the center of the world, we ask them to perform the same **A-pose** (a standard pose) to align the joints. To construct UDP, we remove the original texture and overwrite the color (r, g, b) of each vertex with a landmark, which is currently the world coordinate (x, y, z) , as shown in Figure 2. When the anime body changes its pose, the vertex on the mesh may move to a new position in the world coordinate system, but the landmark at the corresponding body part will remain the same color, shown in the middle of Figure 1.

To avoid the difficulty of down-sampling and processing meshes, we convert the modified meshes into 2D images,



Figure 3: Random characters with random backgrounds

which are friendly to CNNs. This is done by introducing a camera, culling on occluded faces, and projecting only the faces visible from the camera into an image. The resulting UDP representation is a $H \times W \times 4$ shaped image recorded in floating-point numbers ranging from 0 to 1. The four channels include three body landmark encodings and one occupancy for indicating whether the pixel is on the body.

Three properties of UDP could alleviate the difficulties when creating images of 2D animation:

- 1) UDP is a detailed 3D pose representation since every tiny piece of surface on the anime body could be automatically assigned with a unique encoding without hand-crafted annotations.
- 2) UDP is a compatible pose representation since the anime characters with similar body shapes will also get out-fits that are consistently pseudo-colorized.
- 3) UDP can be obtained directly in all existing 3D editors, game engines, and many other up-streams.

Data Preparation

As character sheets used in the anime-related industries are not yet available to the computer vision community, we built a dataset containing more than 20,000 hand-drawn anime characters by selecting human-like characters from public datasets (Anonymous, community, and Branwen 2021; Jerry 2017). We manually perform matting to remove the background from the character with the help of the watershed algorithm. We also construct a 2D background dataset containing 4000 images with a similar method.

Manually annotating hand-drawn anime images with UDP involves significant hardship. To alleviate the problem of label scarcity, we further constructed a synthesized dataset from anime-styled 3D meshes.

Finally, We combined the synthesized dataset with the hand-drawn dataset to obtain both high-quality UDP labels and high diversity of hand-drawn styles. We randomly split the whole dataset by a 1/16 ratio into the validation and training sets. The split is on a per-anime-character basis, so the validation set contains characters unseen during training. The whole dataset contains over 700,000 hand-drawn and synthesized images of diverse poses and appearances. We manually exclude content that is not suitable for public display. Random characters with a random background are shown in Figure 3.

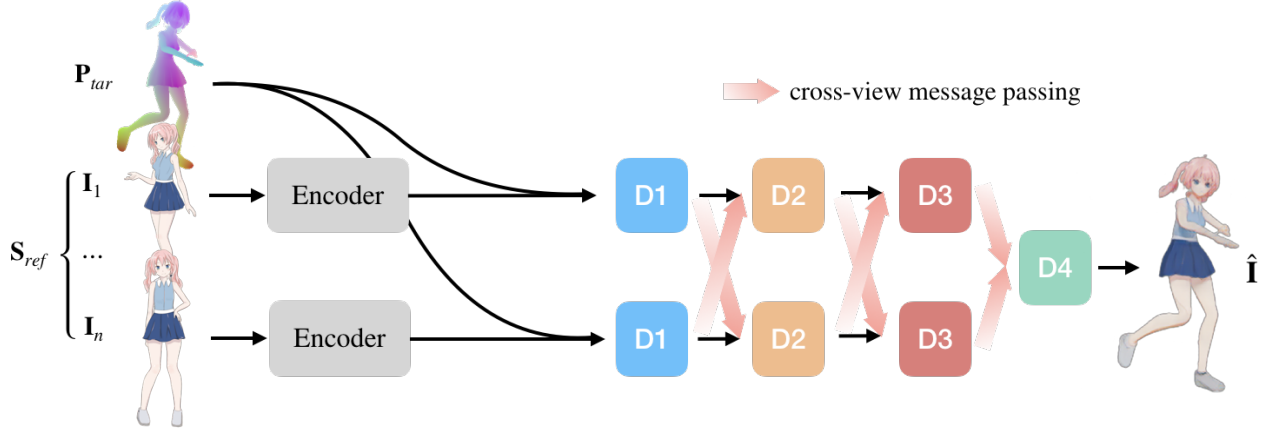


Figure 4: **Overview of CoNR.** Reference images $I_1 \dots I_n \in S_{ref}$ from the input character sheet are fed into CoNR using modified U-Nets (Ronneberger, Fischer, and Brox 2015) as sub-networks. The same UDP representation P_{tar} is resized and concatenated into each scale of the encoder outputs in all sub-networks. Blocks with the same color share weights. “D1 to D4” refers to 4 blocks of the decoder. The sub-networks form a fully connected graph using cross-view message passing. Each block will receive the averaged message from corresponding blocks in all other sub-networks

Collaborative Neural Rendering

Overview. We utilize a collaborative inference for a convolutional neural network named **CINN**, inspired by Point-Net (Qi et al. 2017) and Equivariant-SFM (Moran et al. 2021). CoNR consists of a renderer and an optional UDP detector. Figure 4 shows the pipeline of the proposed approach. CoNR generates a character image of the desired pose, taking the UDP representation \hat{P}_{tar} of the target pose and a character sheet S_{ref} , as the inputs. When generating more than one pose, we feed different UDPs and keep the same reference character sheet.

The input UDP representation can be produced by a UDP detector from reference images or videos. For interactive applications like games, the existing physics engine can be used as a drop-in replacement for the UDP detector to compute body and cloth dynamics for the anime character directly.

Renderer. We apply the following modifications to the U-Net (Ronneberger, Fischer, and Brox 2015):

- 1) As shown in Figure 4, we rescaled UDP with the nearest-sampling method, and concatenate UDP to each block of the decoder. This UDP input strategy is to reuse the results of the encoder and further allow high efficient inference when there are multiple target UDPs, for example, when generating an animation video of a character.
- 2) Due to the spatial misalignment of the local branch and the remote branch, we use flow fields to align the features. Specifically, as inspired by (Dai et al. 2017; Dosovitskiy et al. 2015; Huang et al. 2022), we approximate optical flow as two channels, and warp the features of other channels according to the estimated flow. This operator enhances the long-range look-up ability for CINN.
- 3) We used CINN method in the decoders of the network. We split the original up-sampling output feature channels by half, one as the remote branch and the other for the local branch. First, we warp the features on the remote branches

to align the local features. Then the output features from all remote branches are averaged and concatenated with the encoder output, then fed into the next block (illustrated in Appendix). The last decoder block will collect averaged output features from all previous decoder blocks in all branches and output the final RGB image \hat{I}_{tar} .

UDP Detector. While training with synthesized dataset, UDP \hat{P}_{tar} can be directly obtained. As for hand-drawn dataset, we design a UDP Detector to estimate UDPs \hat{P}_{tar} from hand-drawn images. The UDP Detector is a simple U-Net (Ronneberger, Fischer, and Brox 2015) consists of a ResNet-50 (R50) (He et al. 2016) encoder and a decoder with 5 residual blocks. It is trained jointly with the renderer in an end-to-end manner. We share the weight of the renderer’s encoder and UDP Detector’s encoder.

Experiments

Training Strategy

We train CoNR models of m sub-networks (views) on our dataset. To create one training sample, we randomly select a character and then randomly select $m + 1$ arbitrary poses. These images are split as m character sheet inputs $I_1 \dots I_m \in S_{ref}$ and one image of the target pose as the ground truth of CoNR’s final output.

We paste them onto k random backgrounds and feed them into the UDP detector. We use the average of the k UDP detection results of the same target pose, $\hat{P}_{tar} = 1/k \sum_{j=1}^k \hat{P}_j$, as the final UDP detection results. We compute losses at both the output of the detector and the end of the CoNR pipeline. We use L1 loss on the landmark encodings and BCE loss on the mask to train the detector if the ground truth is available:

$$\mathcal{L}_{udp} = \|\hat{P}_{tar} - P_{tar}^{GT}\|_1, \quad (2)$$

Setting	112K iter		224K iter	
	\mathcal{L}_{photo}	LPIPS	\mathcal{L}_{photo}	LPIPS
$m = 1, n = 1$	0.0247	0.0832	0.0238	0.0801
$m = 4, n = 1$	0.0249	0.0865	0.0237	0.0827
$m = 1, n = 4$	0.0219	0.0798	0.0211	0.0764
$m = 4, n = 4$	0.0187	0.0659	0.0179	0.0612

Table 1: **Comparison on the number of input reference images.** We use character sheets of m reference images to train the CoNR model, and then use character sheets of n reference images to evaluate the trained model

$$\mathcal{L}_{mask} = BCE(\hat{P}_{tar_mask}, P_{tar_mask}^{GT}). \quad (3)$$

We use a consistency loss \mathcal{L}_{cons} by computing the standard deviation of k UDP detector outputs:

$$\mathcal{L}_{cons} = \sqrt{\frac{1}{k-1} \sum_{j=1}^k (\hat{P}_j - \hat{P}_{tar})^2}. \quad (4)$$

At the end of the collaborated renderer, we use L1 loss and feature loss (Ledig et al. 2017) which is based on a pre-trained 19-layer VGG network to supervise the reconstruction in the desired target pose, denoted as L_{photo} and L_{vgg} . The UDP detector and renderer are trained end-to-end simultaneously. The total loss function is the sum of all these losses:

$$\mathcal{L} = \mathcal{L}_{udp} + \mathcal{L}_{cons} + \mathcal{L}_{mask} + \mathcal{L}_{photo} + \alpha \mathcal{L}_{vgg}. \quad (5)$$

where the hyper-parameters of feature loss are from previous work (Zhang, Ng, and Chen 2018).

Our model is optimized by AdamW (Loshchilov and Hutter 2019) with weight decay 10^{-4} for 224K iterations. We choose $m = 4, k = 4$ during training unless otherwise specified. The training process uses a batch size of 24 with all input resolutions set to 256×256 . Model training takes about three weeks on four GPUs.

Result

For quantitative evaluation, we measure the losses on the validation split. Additionally, we use LPIPS (Zhang et al. 2018) to measure the perceptual image quality.

Inference Visual Effects. CoNR can cope with the diverse styles of anime, including differences between synthesized and hand-drawn images. Figure 5 list some random CoNR outputs on the evaluation split. With the same character sheet input S_{ref} , we replaced the provided UDP P_{tar} , and the results of CoNR changed accordingly. Notably, CoNR goes beyond a naive correspondence by absolute UDP value (transfer between different cloths).

Effectiveness of the Collaboration. Unlike most previous methods for similar tasks that allow only one reference image as input, CoNR uses a dynamically-sized set of reference inputs during training and inference.

Table 1 shows that using an additional number of views $m > 1$ during training will enhance the accuracy of generated images. On the opposite, removing images from the



Figure 5: **First row:** Inference results on validation dataset. **Second row:** Inference results with the same character sheet input S_{ref} on different body structure P_{tar}

character sheet will reduce the coverage of the body surface. When CoNR is trained with $m = 1$, the provided character sheets do not allow a reasonable solution, such as giving the character's backside and forcing the model to imagine the frontal side. In this case, the photo-metric reconstruction and feature losses may encourage the network to learn the wrong solution. Therefore even if enough information in the $n > 1$ images is provided during inference, the network may not generate the target image accurately. Similarly, keeping $m = 4$ while reducing the number of inference views ($n = 1$) will also harm the quality of the resulting image.

Adding additional views during inference will enhance the quality of the generated images, as shown in Figure 6. CoNR can leverage information distributed across all images without favoring the first m inputs. This allows CoNR to scale seamlessly from image synthesis, when only a few shots of the character are given, to image interpolating when a lot of footage of a character is available. The example in Figure 6 shows the behavior of CoNR when it does not have enough information to draw missing parts correctly during the inference. Even if very few reference image is provided, the target pose that finds a similar reference in the character sheets will be accurate, as expected. Users can also iterate on the results and feed them back into CoNR to accelerate anime production.

Comparison with Related Work

As CoNR provides a baseline for a new task, we admit that direct comparison with related works can either be impossible or unfair. We still try to include comparisons, only to show how our task is related to other existing tasks.

Human Pose Synthesis. We compare the results produced by CoNR to a real-world digital human system (Liu et al. 2021) using the same target poses¹ as used in their demo. We use two character sheets² with both pose and appearance unseen during training. One contains the same 4 images as

¹Video from download. impersonator.org/iper_plus_plus_latest-samples.zip

²One anime character from www.youtube.com/watch?v=m6k-8t8yEvvE and another character illustrated by an amateur artist.

Character Sheets



Figure 6: **Effectiveness of the collaboration.** We perform a reconstruction test with random video in the wild, with unseen pose and appearance. The last row shows 8 ground truth frames $I_j^{GT} \in S_{vid}^{GT}$ from a video. The first three rows show the inputs and outputs of CoNR. The used subsets of character sheet $S_{ref} \subset S_{vid}^{GT}$ are marked using the blue background. Generated images for novel poses are marked using the red background

Setting	112K iter		224K iter	
	\mathcal{L}_{udp}	\mathcal{L}_{mask}	\mathcal{L}_{udp}	\mathcal{L}_{mask}
Original U-Net	0.1247	0.0856	Fail	Fail
U-Net+R34	0.1051	0.1068	0.1004	0.0747
U-Net+R50	0.0969	0.0792	0.0971	0.0736

Table 2: **Ablation on UDP Detector with different backbones**

in Figure 1, the other character sheet taken from a random YouTube video contains $I_{1 \sim 5}$ as used in Figure 6. Figure 7 indicates that the long skirt prevents a high accuracy estimation of the leg joints and that parametric 3D human models like SMPL may not handle the body shape of anime characters correctly. CoNR can produce images at desired target poses with better quality.

Image synthesis pipelines starting with human pose representations are theoretically inapplicable on anime data, as the character’s diverse body structure, clothing, and accessories cannot be reasonably represented. Using human pose synthesis methods in anime, we may lose artistic control over garments and fine details, which is crucial in anime creation workflows.

Style Transfer. Style transfer typically refers to applying a learned style from a certain domain (anime images) to the input image taken from the other domain (real-world images) (Chen, Liu, and Chen 2019; Wang and Yu 2020b). The models usually treat the target domain as a kind of style and require extensive training to remember the style. Some

U-Net	Warping	CINN	R50	224K iter	
				\mathcal{L}_{photo}	LPIPS
✓				0.0311	0.1038
✓	✓			0.0308	0.1036
✓		✓	✓	0.0286	0.0977
✓	✓	✓		0.0180	0.0612
✓	✓	✓	✓	0.0179	0.0612

Table 3: **Ablation on Renderer.** The warping operation over the output features of each decoder block. All comparisons are done with character sheets of $m = 4$ images

methods use a single image to provide a style hint during the inference. For example, one could use Swapping Auto Encoders (Park et al. 2020), a recent style-transfer method to swap the textures or body structures between two characters. Although the model has a lot of parameters (3× the size of CoNR), our comparison shows that it is still not enough to remember and reproduce the diverse sub-styles of the textures, pose, and body structure in the domain of anime.

CoNR, as a neural rendering method, can also be used to achieve results similar to what style transfer methods could provide when running a textured image at the reference pose through the UDP detector, as shown in 4. The CoNR inference pipeline for the anime (or game) production will usually be without the UDP detector.

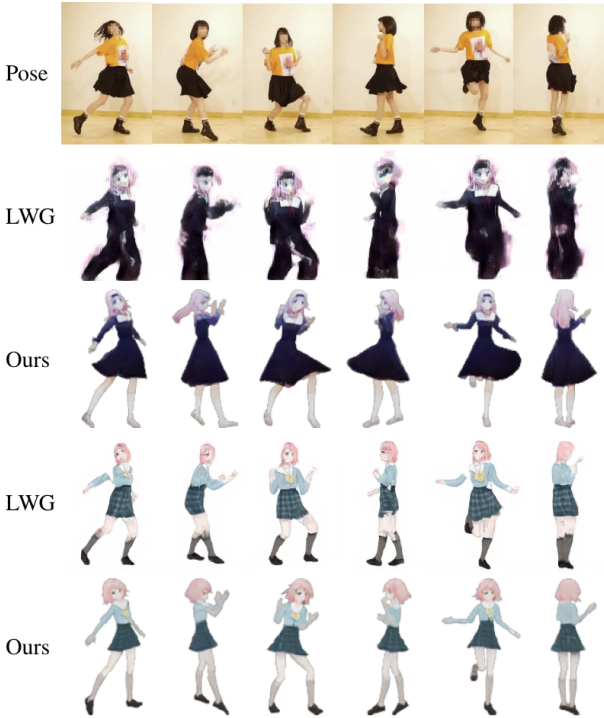


Figure 7: Comparison with the SMPL-based method. We compare the results of our method with the results of Liquid Warpping GAN (LWG) (Liu et al. 2021) when trying to resemble the target poses. **The real person in the first row is only used to show the pose.** Further diagnosis shows that parametric 3D human models like SMPL may not represent anime’s diverse clothing and body shape. The short skirt of the second character is tightened on the legs instead of sagging naturally

Ablation Study

We perform ablation studies on the UDP detector, renderer, and loss functions. Table 2 shows that UDP representation can be inferred from images using a U-Net (Ronneberger, Fischer, and Brox 2015). An original U-Net, which takes a concatenated tensor of 4 reference images and the target UDP as the input, does not provide acceptable results on this task, as shown in Table 3. The proposed CoNR method with both the feature warping and the CINN method significantly increases the performance, thus establishing a stronger baseline for the proposed task. We further ablate the loss functions in Table 4.

Limitations

CoNR is unable to model the environmental lighting effects. The inputs of CoNR can not provide any information about the environmental or contextual information that could be utilized to infer lighting effects. Users may have to look for sketch relighting techniques (Zheng, Li, and Bargteil 2020; Gao et al. 2018; Su et al. 2018).

CoNR is unable to model the dynamics of the character. The CoNR model accepts target poses detected from



Figure 8: Comparision between detection results of hand-drawn anime character images using OpenPose (Cao et al. 2019), the UDP detector and SMPLify (Bogo et al. 2016). The images are from the validation split of the hand-drawn dataset (Anonymous, community, and Branwen 2021) with the corresponding ID number. The detected SMPL body can not fully handle the diverse body shapes of anime characters. UDP detector produces relatively reasonable results

Setting	224K iter			
	\mathcal{L}_{udp}	\mathcal{L}_{mask}	\mathcal{L}_{photo}	LPIPS
w/o \mathcal{L}_{mask}	0.162	0.880	-	-
w/o \mathcal{L}_{photo}	-	-	0.023	0.084
w/o \mathcal{L}_{vgg}	-	-	0.028	0.158
Baseline	0.097	0.079	0.019	0.066

Table 4: Ablation on loss functions

a video of a character with a body shape similar to S_{ref} , and could inherit the dynamics. However, it requires such a pose sequence beforehand. To bypass the UDP detector, we can rely on additional technologies like garment captures (Bradley et al. 2008), physics simulations (Baraff and Witkin 1998), learning-based methods (Wang et al. 2019; Tiwari et al. 2021) or existing 3D animation workflows to obtain a synthesized UDP P_{tar} . CoNR focuses on the rendering task. Obtaining a suitable 3D mesh with all the body parts rigged and all clothing computed with proper dynamics is beyond the scope of this paper. Using P_{tar} from an inappropriate body shape may lead to incorrect CoNR results, as shown in Figure 5.

The dataset may not fully follow the distribution of anime characters in the wild. The collected dataset contains only human-like anime characters from 2014 to 2018. As the character meshes are aligned using joints, the models trained on this dataset may not be applied to animal-like characters. Research on broader datasets will be the future work.

Conclusion

This work introduces a new task to render anime character images with the desired pose from multiple images in character sheets. We developed a simple feed-forward baseline method, CoNR. The effectiveness of the method is encouraging. We hope the method and the datasets presented in this paper will inspire further research.

References

Alldieck, T.; Pons-Moll, G.; Theobalt, C.; and Magnor, M. 2019. Tex2shape: Detailed full human body geometry from a single image. In *Proceedings of the IEEE International Conference on Computer Vision (ICCV)*.

Anonymous; community, D.; and Branwen, G. 2021. Danbooru2020: A Large-Scale Crowdsourced and Tagged Anime Illustration Dataset. <https://www.gwern.net/Danbooru2020>. Accessed: DATE.

aydao. 2021. Website: This anime does not exist. <https://thisanimedoesnotexist.ai>.

Baraff, D.; and Witkin, A. 1998. Large steps in cloth simulation. In *Proceedings of the 25th annual conference on Computer graphics and interactive techniques*, 43–54.

Blanz, V.; and Vetter, T. 1999. A morphable model for the synthesis of 3D faces. In *Proceedings of the 26th annual conference on Computer graphics and interactive techniques*, 187–194.

Bogo, F.; Kanazawa, A.; Lassner, C.; Gehler, P.; Romero, J.; and Black, M. J. 2016. Keep it SMPL: Automatic estimation of 3D human pose and shape from a single image. In *European conference on computer vision (ECCV)*.

Bradley, D.; Popa, T.; Sheffer, A.; Heidrich, W.; and Boubekeur, T. 2008. Markerless garment capture. In *ACM SIGGRAPH*.

Cao, Z.; Hidalgo, G.; Simon, T.; Wei, S.-E.; and Sheikh, Y. 2019. OpenPose: realtime multi-person 2D pose estimation using Part Affinity Fields. *IEEE transactions on pattern analysis and machine intelligence (TPAMI)*, 43(1): 172–186.

Chan, C.; Ginosar, S.; Zhou, T.; and Efros, A. A. 2019. Everybody dance now. In *Proceedings of the IEEE International Conference on Computer Vision (ICCV)*.

Chen, J.; Liu, G.; and Chen, X. 2019. AnimeGAN: A novel lightweight gan for photo animation. In *International Symposium on Intelligence Computation and Applications*, 242–256. Springer.

Chou, C.-L.; Chen, C.-Y.; Hsieh, C.-W.; Shuai, H.-H.; Liu, J.; and Cheng, W.-H. 2021. Template-Free Try-On Image Synthesis via Semantic-Guided Optimization. *IEEE Transactions on Neural Networks and Learning Systems (TNNLS)*.

Dai, J.; Qi, H.; Xiong, Y.; Li, Y.; Zhang, G.; Hu, H.; and Wei, Y. 2017. Deformable convolutional networks. In *Proceedings of the IEEE International Conference on Computer Vision (ICCV)*.

Dosovitskiy, A.; Fischer, P.; Ilg, E.; Hausser, P.; Hazirbas, C.; Golkov, V.; Van Der Smagt, P.; Cremers, D.; and Brox, T. 2015. Flownet: Learning optical flow with convolutional networks. In *Proceedings of the IEEE International Conference on Computer Vision (ICCV)*.

Gafni, O.; Ashual, O.; and Wolf, L. 2021. Single-Shot Freestyle Dance Reenactment. In *Proceedings of the IEEE Conference on Computer Vision and Pattern Recognition (CVPR)*.

Gao, C.; Shih, Y.; Lai, W.-S.; Liang, C.-K.; and Huang, J.-B. 2020. Portrait Neural Radiance Fields from a Single Image. *arXiv preprint arXiv:2012.05903*.

Gao, Z.; Yonetsuji, T.; Takamura, T.; Matsuoka, T.; and Naradowsky, J. 2018. Automatic Illumination Effects for 2D Characters. In *NIPS Workshop on Machine Learning for Creativity and Design*.

Gokaslan, A.; Ramanujan, V.; Ritchie, D.; Kim, K. I.; and Tompkin, J. 2018. Improving shape deformation in unsupervised image-to-image translation. In *Proceedings of the European Conference on Computer Vision (ECCV)*.

Gooch, B.; and Gooch, A. 2001. *Non-photorealistic rendering*. AK Peters/CRC Press.

Güler, R. A.; Neverova, N.; and Kokkinos, I. 2018. Densepose: Dense human pose estimation in the wild. In *Proceedings of the IEEE Conference on Computer Vision and Pattern Recognition (CVPR)*.

He, K.; Zhang, X.; Ren, S.; and Sun, J. 2016. Deep residual learning for image recognition. In *Proceedings of the IEEE Conference on Computer Vision and Pattern Recognition (CVPR)*.

He, Z.; Kan, M.; and Shan, S. 2021. EigenGAN: Layer-Wise Eigen-Learning for GANs. In *Proceedings of the IEEE International Conference on Computer Vision (ICCV)*.

Huang, Z.; Zhang, T.; Heng, W.; Shi, B.; and Zhou, S. 2022. Real-Time Intermediate Flow Estimation for Video Frame Interpolation. In *Proceedings of the European Conference on Computer Vision (ECCV)*.

Huang, Z.; Zhou, S.; and Heng, W. 2019. Learning to Paint With Model-Based Deep Reinforcement Learning. In *Proceedings of the IEEE International Conference on Computer Vision (ICCV)*.

Jerry, L. 2017. Pixiv Dataset. https://github.com/jerryli27/pixiv_dataset.

Jin, Y.; Zhang, J.; Li, M.; Tian, Y.; Zhu, H.; and Fang, Z. 2017. Towards the Automatic Anime Characters Creation with Generative Adversarial Networks. In *NIPS Workshop on Machine Learning for Creativity and Design*.

Khungurn, P.; and Chou, D. 2016. Pose estimation of anime/manga characters: a case for synthetic data. In *Proceedings of the 1st International Workshop on coMics ANalysis, Processing and Understanding*, 1–6.

Ledig, C.; Theis, L.; Huszár, F.; Caballero, J.; Cunningham, A.; Acosta, A.; Aitken, A.; Tejani, A.; Totz, J.; Wang, Z.; et al. 2017. Photo-realistic single image super-resolution using a generative adversarial network. In *Proceedings of the IEEE Conference on Computer Vision and Pattern Recognition (CVPR)*.

Li, M.; Jin, Y.; and Zhu, H. 2021. Surrogate Gradient Field for Latent Space Manipulation. In *Proceedings of the IEEE Conference on Computer Vision and Pattern Recognition (CVPR)*.

Liu, W.; Piao, Z.; Min, J.; Luo, W.; Ma, L.; and Gao, S. 2019. Liquid warping gan: A unified framework for human motion imitation, appearance transfer and novel view synthesis. In *Proceedings of the IEEE International Conference on Computer Vision (ICCV)*.

Liu, W.; Piao, Z.; Tu, Z.; Luo, W.; Ma, L.; and Gao, S. 2021. Liquid Warping GAN with Attention: A Unified Framework for Human Image Synthesis. *IEEE Transactions on Pattern Analysis and Machine Intelligence (TPAMI)*.

Loper, M.; Mahmood, N.; Romero, J.; Pons-Moll, G.; and Black, M. J. 2015. SMPL: A skinned multi-person linear model. *ACM transactions on graphics (TOG)*, 34(6): 1–16.

Loshchilov, I.; and Hutter, F. 2019. Decoupled weight decay regularization. In *Proceedings of the International Conference on Learning Representations (ICLR)*.

Mildenhall, B.; Srinivasan, P. P.; Tancik, M.; Barron, J. T.; Ramamoorthi, R.; and Ng, R. 2020. Nerf: Representing scenes as neural radiance fields for view synthesis. In *Proceedings of the European Conference on Computer Vision (ECCV)*.

Moran, D.; Koslowsky, H.; Kasten, Y.; Maron, H.; Galun, M.; and Basri, R. 2021. Deep Permutation Equivariant Structure from Motion. In *Proceedings of the IEEE/CVF International Conference on Computer Vision (ICCV)*.

Neverova, N.; Novotny, D.; Szafraniec, M.; Khalidov, V.; Labatut, P.; and Vedaldi, A. 2020. Continuous surface embeddings. In *Advances in Neural Information Processing Systems (NIPS)*.

Park, T.; Zhu, J.-Y.; Wang, O.; Lu, J.; Shechtman, E.; Efros, A.; and Zhang, R. 2020. Swapping autoencoder for deep image manipulation. *Advances in Neural Information Processing Systems*, 33: 7198–7211.

Peng, S.; Dong, J.; Wang, Q.; Zhang, S.; Shuai, Q.; Zhou, X.; and Bao, H. 2021. Animatable Neural Radiance Fields for Modeling Dynamic Human Bodies. In *Proceedings of the IEEE International Conference on Computer Vision (ICCV)*.

Pumarola, A.; Corona, E.; Pons-Moll, G.; and Moreno-Noguer, F. 2021. D-nerf: Neural radiance fields for dynamic scenes. In *Proceedings of the IEEE Conference on Computer Vision and Pattern Recognition (CVPR)*.

Qi, C. R.; Su, H.; Mo, K.; and Guibas, L. J. 2017. Pointnet: Deep learning on point sets for 3d classification and segmentation. In *Proceedings of the IEEE conference on computer vision and pattern recognition (CVPR)*.

Radford, A.; Kim, J. W.; Hallacy, C.; Ramesh, A.; Goh, G.; Agarwal, S.; Sastry, G.; Askell, A.; Mishkin, P.; Clark, J.; et al. 2021. Learning transferable visual models from natural language supervision. In *International Conference on Machine Learning*, 8748–8763. PMLR.

Ronneberger, O.; Fischer, P.; and Brox, T. 2015. U-net: Convolutional networks for biomedical image segmentation. In *International Conference on Medical image computing and computer-assisted intervention (MICCAI)*.

Sarkar, K.; Mehta, D.; Xu, W.; Golyanik, V.; and Theobalt, C. 2020. Neural re-rendering of humans from a single image. In *European Conference on Computer Vision (ECCV)*.

Shen, Y.; and Zhou, B. 2021. Closed-form factorization of latent semantics in gans. In *Proceedings of the IEEE/CVF Conference on Computer Vision and Pattern Recognition (CVPR)*.

Siarohin, A.; Lathuilière, S.; Tulyakov, S.; Ricci, E.; and Sebe, N. 2019. First order motion model for image animation. In *Advances in Neural Information Processing Systems (NIPS)*.

Siarohin, A.; Woodford, O. J.; Ren, J.; Chai, M.; and Tulyakov, S. 2021. Motion representations for articulated animation. In *Proceedings of the IEEE Conference on Computer Vision and Pattern Recognition (CVPR)*.

Siyao, L.; Zhao, S.; Yu, W.; Sun, W.; Metaxas, D.; Loy, C. C.; and Liu, Z. 2021. Deep Animation Video Interpolation in the Wild. In *Proceedings of the IEEE Conference on Computer Vision and Pattern Recognition (CVPR)*.

Su, H.; Niu, J.; Liu, X.; Cui, J.; and Wan, J. 2021. Vectorization of Raster Manga by Deep Reinforcement Learning. *arXiv preprint arXiv:2110.04830*.

Su, W.; Du, D.; Yang, X.; Zhou, S.; and Fu, H. 2018. Interactive sketch-based normal map generation with deep neural networks. *Proceedings of the ACM on Computer Graphics and Interactive Techniques*, 1(1): 1–17.

Tiwari, G.; Sarafianos, N.; Tung, T.; and Pons-Moll, G. 2021. Neural-GIF: Neural generalized implicit functions for animating people in clothing. In *Proceedings of the IEEE International Conference on Computer Vision (ICCV)*.

Tseng, H.-Y.; Fisher, M.; Lu, J.; Li, Y.; Kim, V.; and Yang, M.-H. 2020. Modeling artistic workflows for image generation and editing. In *Proceedings of the European Conference on Computer Vision (ECCV)*.

Wang, T.-C.; Mallya, A.; and Liu, M.-Y. 2021. One-shot free-view neural talking-head synthesis for video conferencing. In *Proceedings of the IEEE Conference on Computer Vision and Pattern Recognition (CVPR)*.

Wang, T. Y.; Shao, T.; Fu, K.; and Mitra, N. J. 2019. Learning an intrinsic garment space for interactive authoring of garment animation. *ACM Transactions on Graphics (TOG)*, 38(6): 1–12.

Wang, X.; and Yu, J. 2020a. Learning to cartoonize using white-box cartoon representations. In *Proceedings of the IEEE Conference on Computer Vision and Pattern Recognition (CVPR)*.

Wang, X.; and Yu, J. 2020b. Learning to cartoonize using white-box cartoon representations. In *Proceedings of the IEEE Conference on Computer Vision and Pattern Recognition (CVPR)*.

Yao, P.; Fang, Z.; Wu, F.; Feng, Y.; and Li, J. 2019. Densebody: Directly regressing dense 3d human pose and shape from a single color image. *arXiv preprint arXiv:1903.10153*.

Yoon, J. S.; Liu, L.; Golyanik, V.; Sarkar, K.; Park, H. S.; and Theobalt, C. 2021. Pose-Guided Human Animation from a Single Image in the Wild. In *Proceedings of the IEEE Conference on Computer Vision and Pattern Recognition (CVPR)*.

Zanfir, M.; Popa, A.-I.; Zanfir, A.; and Sminchisescu, C. 2018. Human appearance transfer. In *Proceedings of the IEEE Conference on Computer Vision and Pattern Recognition (CVPR)*.

Zhang, R.; Isola, P.; Efros, A. A.; Shechtman, E.; and Wang, O. 2018. The unreasonable effectiveness of deep features as a perceptual metric. In *Proceedings of the IEEE Conference on Computer Vision and Pattern Recognition (CVPR)*.

Zhang, S.-H.; Chen, T.; Zhang, Y.-F.; Hu, S.-M.; and Martin, R. R. 2009. Vectorizing cartoon animations. *IEEE Transactions on Visualization and Computer Graphics*, 15(4): 618–629.

Zhang, X.; Ng, R.; and Chen, Q. 2018. Single image reflection separation with perceptual losses. In *Proceedings of the IEEE Conference on Computer Vision and Pattern Recognition (CVPR)*.

Zheng, Q.; Li, Z.; and Bargteil, A. 2020. Learning to Shadow Hand-drawn Sketches. In *Proceedings of the IEEE Conference on Computer Vision and Pattern Recognition (CVPR)*.

Appendix

Experiment Details

The synthesized part of the dataset contains multiple-pose and multiple-view images. Each of them is paired with UDP annotations. A randomly-sampled subset of 3D mesh data obtained in the same way as in (Khungurn and Chou 2016) was used in this work, which contains 2,000 anime characters with more than 200 poses. The scope of permissions was confirmed before using existing assets in this work. The contribution in this work is mostly about years of manual data clean-up, which includes converting mesh formats, restructuring the bone hierarchy, and aligning the A-poses before synthesizing RGB images for each pose, and their corresponding UDPs with MikuMikuDance (MMD) software.

The mixed dataset also contains unlabeled hand-drawn samples and one-shot samples, *i.e.* characters with the only single available pose, which are randomly sampled from existing datasets (Anonymous, community, and Branwen 2021; Jerry 2017). We make full use of the mixed data by performing semi-supervised learning. For the detector, we skip the \mathcal{L}_{udp} as we do not have ground truth but keep the \mathcal{L}_{cons} to ensure the detector makes the same prediction of the same character under k random augmentations. As for the renderer, we have to reuse the image of the same pose multiple times to fill all the m views if the provided images in the character sheet are not enough. Random-crop augmentation is applied to $\mathbf{I}_m \in \mathbf{S}_{ref}$, $\hat{\mathbf{P}}_{tar}$ and \mathbf{I}_{tar}^{gt} . With the random-crop augmentation, in order to generate the image of body parts in the right position, CoNR has to learn a cross-modality feature matching instead of a trivial solution by simply selecting one of the provided images as the output.

Ablation on Message Passing

We perform ablations on the number of messages passing for the CoNR. More ghosting can be observed when sub-networks communicate less than three times.



Messaging	112k iter		224k iter	
	\mathcal{L}_{photo}	LPIPS	\mathcal{L}_{photo}	LPIPS
1 time	0.028	0.107	0.026	0.099
3 times	0.018	0.065	0.017	0.061

Comparison with Style Transfer method

To best of our knowledge, fusion of pose and texture for virtual character cannot be solved directly by implicit style transfer. As shown in Figure 10, SwapAE fails in this scene.

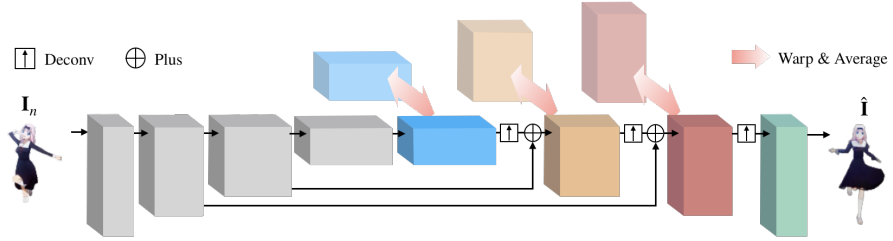


Figure 9: **Sub-network structure of CoNR.** Every input $I_n \in S_{ref}$ goes into a U-Net shaped sub-network. The warping and averaging operation are performed on the output of every decoder block. The semi-transparent blocks represent corresponding blocks in all other sub-networks. Blocks with the same color share weights. Each block in a sub-network would pass part of the outputs as messages to corresponding successive blocks in all other sub-networks, in addition to forwarding outputs to its following blocks in the current sub-network. The path of UDP is omitted.



Figure 10: **Evaluation results of Swapping Autoencoder (SwapAE) (Park et al. 2020) for Deep Image Manipulation.** We trained a Pytorch implementation of SwapAE (Park et al. 2020) with pairs of images of different characters in our dataset. This figure, from the first to the last row, shows (a) the target pose image, (b) the reference image, (c) pose of **a** and texture of **b**, fused by SwapAE, (d) pose of **b** and texture of **a**, fused by SwapAE